



# AMERICAN METEOROLOGICAL SOCIETY

*Bulletin of the American Meteorological Society*

## **EARLY ONLINE RELEASE**

This is a preliminary PDF of the author-produced manuscript that has been peer-reviewed and accepted for publication. Since it is being posted so soon after acceptance, it has not yet been copyedited, formatted, or processed by AMS Publications. This preliminary version of the manuscript may be downloaded, distributed, and cited, but please be aware that there will be visual differences and possibly some content differences between this version and the final published version.

The DOI for this manuscript is doi: 10.1175/BAMS-D-13-00171.1

The final published version of this manuscript will replace the preliminary version at the above DOI once it is available.

If you would like to cite this EOR in a separate work, please use the following full citation:

Adams, D., R. Fernandes, K. Holub, S. Gutman, H. Barbosa, L. Machado, A. Calheiros, R. Bennett, R. Kursinski, L. Sapucci, C. DeMets, G. Chagas, A. Arellano, N. Filizola, A. Amorim, R. Araujo, L. Assuncao, G. Cirino, T. Pauliquevis, B. Portela, A. Sa, J. Sousa, and L. Tanaka, 2015: The Amazon Dense GNSS Meteorological Network: A New Approach for Examining Water Vapor and Deep Convection Interactions in the Tropics. *Bull. Amer. Meteor. Soc.* doi:10.1175/BAMS-D-13-00171.1, in press.



1     **The Amazon Dense GNSS Meteorological Network: A New**  
2     **Approach for Examining Water Vapor and Deep Convection**  
3     **Interactions in the Tropics**

4                     **DAVID K. ADAMS \***

*Centro de Ciencias de la Atmósfera, Universidad Nacional Autónoma de México, México*

**RUI M. S. FERNANDES**

*Instituto D. Luíz, Universidade da Beira Interior, Covilhã, Portugal and*

*Faculty of Aerospace Engineering, Delft University of Technology, Delft, The Netherlands*

5                     **KIRK L. HOLUB**

*Office of Oceanic and Atmospheric Research, National Oceanic and Atmospheric Administration, Boulder, CO, USA*

6                     **SETH I. GUTMAN**

*Office of Oceanic and Atmospheric Research, National Oceanic and Atmospheric Administration, Boulder, CO, USA*

7                     **HENRIQUE M. J. BARBOSA**

*Instituto de Física, Universidade de São Paulo, São Paulo, Brazil*

8                     **LUIZ A. T. MACHADO**

*Centro de Previsão de Tempo e Estudos Climáticos, Instituto Nacional de Pesquisas Espaciais, São Paulo, Brazil*

9

ALAN J. P. CALHEIROS

*Centro de Previsão de Tempo 1e Estudos Climáticos, Instituto Nacional de Pesquisas Espaciais, São Paulo, Brazil*

10

RICHARD A. BENNETT

*Department of Geosciences, University of Arizona, Tucson, USA*

11

E. ROBERT KURSINSKI

*Moog Advanced Missions and Science, Golden, CO, USA*

12

LUIZ F. SAPUCCI

*Centro de Previsão de Tempo e Estudos Climáticos, Instituto Nacional de Pesquisas Espaciais, São Paulo, Brazil*

13

CHARLES DEMETS

*Department of Geoscience, University of Wisconsin, Madison, WI, USA*

14

GLAYSON F. B. CHAGAS

*Programa de Pós Graduação em Clima e Ambiente, Universidade do Estado do Amazonas, Manaus, Amazonas, Brazil*

15

AVE ARELLANO

*Department of Atmospheric Sciences, University of Arizona, Tucson, USA*

16

NAZIANO FILIZOLA

*Departamento de Geografia, Universidade Federal do Amazonas, Manaus, Amazonas, Brazil*

17

ALCIÉLIO A. AMORIM ROCHA

*Programa de Pós Graduação em Clima e Ambiente, Universidade do Estado do Amazonas, Manaus, Amazonas, Brazil*

18

ROSIMEIRE ARAÚJO SILVA

*Programa de Pós Graduação em Clima e Ambiente, Universidade do Estado do Amazonas, Manaus, Amazonas, Brazil*

19

LILIA M. F. ASSUNÇÃO

*Programa de Pós Graduação em Clima e Ambiente, Universidade do Estado do Amazonas, Manaus, Amazonas, Brazil*

20

GLAUBER G. CIRINO

*Programa de Pós Graduação em Clima e Ambiente, Universidade do Estado do Amazonas, Manaus, Amazonas, Brazil*

21

THEOTONIO PAULIQUEVIS

*Departamento de Ciências Exatas e da Terra, Universidade Federal de São Paulo, Diadema, Brazil*

22

BRUNO T. T. PORTELA

*Programa de Pós Graduação em Clima e Ambiente, Universidade do Estado do Amazonas, Manaus, Amazonas, Brazil*

23

ANDRÉ SÁ

*Departamento de Engenharia e Tecnologia, Instituto Politécnico da Guarda, Guarda, Portugal and*

*Departamento de Informática, Universidade da Beira Interior, Covilhã, Portugal*

24

JEANNE M. DE SOUSA

*Programa de Pós Graduação em Clima e Ambiente, Universidade do Estado do Amazonas, Manaus, Amazonas, Brazil*

25

LUDMILA M. S. TANAKA

*Programa de Pós Graduação em Clima e Ambiente, Universidade do Estado do Amazonas, Manaus, Amazonas, Brazil*

---

\* *Corresponding author address:* David K. Adams, Centro de Ciencias de la Atmósfera, Universidad Nacional Autónoma de México, Circuito Exterior s/n, Ciudad Universitaria, Del. Coyoacán 04510, México D.F..

## ABSTRACT

27 The complex interactions between water vapor fields and deep atmospheric convection remain  
28 one of the outstanding problems in Tropical Meteorology. The lack of high spatial/temporal  
29 resolution, all-weather observations in the Tropics has hampered progress. Numerical models  
30 have difficulties, for example, in representing the shallow-to-deep convective transition and  
31 the diurnal cycle of precipitation. GNSS (Global Navigation Satellite System) meteorology,  
32 which provides all-weather, high frequency (5 minutes), precipitable water vapor estimates,  
33 can help. The Amazon Dense GNSS Meteorological Network experiment, the first of its kind  
34 ever in the Tropics, was created with the aim of examining water vapor and deep convection  
35 relationships at the mesoscale. This innovative, Brazilian-led international experiment con-  
36 sisted of two mesoscale (100km x 100km) networks: (1) a one-year (April 2011 to April 2012)  
37 campaign (20 GNSS meteorological sites) in and around Manaus, and (2) a 6 week (June  
38 2011) intensive campaign (15 GNSS meteorological sites) in and around Belem, this latter in  
39 collaboration with the CHUVA Project in Brazil. Results presented here from both networks  
40 focus on the diurnal cycle of precipitable water vapor associated with sea breeze convection  
41 in Belem and seasonal and topographic influences in and around Manaus. Ultimately, these  
42 unique observations may serve to initialize, constrain, or validate precipitable water vapor  
43 in high resolution models. These experiments also demonstrate that GNSS meteorology  
44 can expand into logistically difficult regions such as the Amazon. Other GNSS meteorology  
45 networks presently being constructed in the Tropics are summarized.

## 46 1. Capsule

47 The Amazon Dense GNSS Meteorological Network provides high spatial/temporal reso-  
48 lution, all-weather precipitable water vapor for studying the evolution of continental tropical  
49 and sea-breeze convective regimes of Amazonia.

## 50 2. Introduction

51 The meteorology and climate of the equatorial Tropics are dominated by atmospheric  
52 convection, which presents a rather challenging range of spatial and temporal scales to  
53 capture with present-day observational platforms (Mapes and Neale 2011; Moncrieff et al.  
54 2012; Zhang et al. 2013). Over a period of a few hours, shallow convection (order 1-10km  
55 in horizontal scale) can transition to deep precipitating convection (order 10-100km) and  
56 then organize into mesoscale convective systems (order 100-1000km) with lifetimes ranging  
57 from several hours to greater than one day. Furthermore, complex feedbacks exist between  
58 atmospheric convection and the thermodynamic environment, particularly water vapor fields,  
59 in which convection develops (see Sherwood et al. (2009) for a review of convection and water  
60 vapor interactions).

61 Understanding and modeling tropical convection have been hampered by the dearth of  
62 long-term observations resolving the mesoscale. For example, large-scale models where con-  
63 vection is parameterized have poorly represented the diurnal cycle of convective precipitation,  
64 particularly over land, possibly resulting in the degradation of model clouds, radiation fields  
65 and large-scale dynamics (Betts and Jakob 2002a,b; Bechtold et al. 2004). While single  
66 column models and high resolution models (cloud resolving to large eddy simulations) are a  
67 useful tool (Betts and Jakob 2002b; Grabowski and Moncrieff 2004; Grabowski et al. 2006),  
68 they are not a substitute for observations. Many efforts have focused on what controls the  
69 shallow-to-deep convection transition, a process often missing in coarse models with sepa-  
70 rate shallow and deep convection schemes (Betts and Jakob 2002b,a; Grabowski et al. 2006;

71 Kuang and Bretherton 2006; Khairoutdinov and Randall 2006; Waite and Khouider 2010;  
72 Wu et al. 2009; Hohenegger and Stevens 2013). Mechanisms to explain the shallow-to-deep  
73 transition include: cold pool formation (Kuang and Bretherton 2006; Khairoutdinov and  
74 Randall 2006; Schlemmer and Hohenegger 2014), cumulus congestus moistening of the free  
75 troposphere (Waite and Khouider 2010), increasing cloud buoyancy (Wu et al. 2009), and  
76 dynamically forced, large-scale vertical motions and attendant water vapor convergence (Ho-  
77 henegger and Stevens 2013). Whatever the mix of these model-elucidated physical mecha-  
78 nisms, even high resolution models must somehow be evaluated with real-world observations  
79 which, unfortunately, are sorely lacking in the Tropics at the necessary temporal/spatial  
80 scale.

81 Geostationary satellites are the backbone of observational studies of the evolution and  
82 life cycle of tropical convection (Sherwood and Warhlich 1999; Masunaga 2013). Visible and  
83 IR cloud imagery can document the evolution of cumulus fields at high spatial resolution and  
84 adequate temporal resolution (15 to 30 minutes). However, water vapor is more challenging  
85 to measure from space. IR radiometers for measuring column water vapor are limited to  
86 clear-sky conditions while microwave observations, although all-weather, are unreliable over  
87 land and sporadic over water. Long-term, surface-based, mesoscale meteorological networks  
88 thus have a unique role to play. Unfortunately, only brief field campaigns in the continental  
89 Tropics, such as the Amazon, have been carried out due to logistical difficulties (e.g., ABLE  
90 2B, Garstang et al. (1990), TRMM/LBA, Silva-Dias et al. (2002); Betts et al. (2009) and  
91 currently GOAmazon). Global Navigational Satellite System (GNSS) meteorology ( “GPS”,  
92 Global Positioning System being the most commonly used) can help in this regard.

93 For two decades, GNSS/GPS meteorology has offered relatively inexpensive, high fre-  
94 quency ( $\sim 5$  minutes), *all-weather*, “precipitable” or column integrated water vapor (PWV)  
95 values within 1 to 2 mm accuracy compared to radiosondes and radiometers (Bevis et al.  
96 1992; Rocken et al. 1993; Duan et al. 1996; Wolfe and Gutman 2000; Sapucci et al. 2007). A  
97 related space-based technique, GPS radio occultation provides water vapor profiles, but is

98 too infrequent to capture water vapor field evolution at a given location, see (Kursinski et al.  
99 (2000)). Estimation of the effects of cloud liquid/ice water, precipitation and atmospheric  
100 aerosols/dust on GNSS signals can be found in (Solheim et al. 1999). For process-oriented,  
101 mesoscale studies of water vapor/convection interactions, a network of sites is needed. The  
102 GNSS cone of observation has an approximately 10km radius, covering the spatial and tempo-  
103 ral scale at which the shallow-to-deep transition occurs and upscale convective organization  
104 begins (Moncrieff et al. 2012). With GNSS meteorology arranged in a network, mesoscale  
105 convective organization and associated water vapor fields can be documented. Surprisingly,  
106 after two decades, most GNSS studies have focused on the technique itself, validating ra-  
107 diosondes, radiometers or satellite platforms, or as ancillary data for large-scale studies or  
108 numerical weather data assimilation/prediction. Mesoscale, process-oriented GNSS studies  
109 are few, and even less so for the deep Tropics.

110 The Amazon Dense GNSS Meteorological Network (ADGMN) was created to address  
111 these issues of water vapor/convection interactions. In this brief overview of the ADGMN,  
112 we encapsulate the motivations and goals (Section 3) as well as the experimental design  
113 (Section 4) for both the Belem and Manaus networks. An example of the diurnal cycle of  
114 sea-breeze convection for Belem and ideas for future work for this network are presented in  
115 Section 5. Results from the Manaus network (Section 6) also describe the diurnal cycle with  
116 respect to topographic effects and the seasonal evolution given that the data set spans one  
117 year. Prospects for expanding large-scale GNSS networks in the Tropics, specifically in the  
118 Caribbean and Mexico, are then surveyed. A secondary goal is to demonstrate that GNSS  
119 meteorology is viable even in regions fraught with logistical difficulties such as the Amazon.

### 120 **3. The ADGMN: Motivations and Aims**

121 Dense GNSS meteorological networks are not new in Europe (Champollion et al. 2005;  
122 Bastin et al. 2007; Brenot et al. 2013), Japan (Seko et al. 2004) nor the US (Champollion

123 et al. 2009); neither are GNSS studies of deep convection (Mazany et al. 2002; Kursinski  
124 et al. 2008; Brenot et al. 2013). However, the deep tropics offer new challenges as well as  
125 unique weather situations to explore. Establishing any type of meteorological network in the  
126 Amazon is a challenging logistical task as suitable sites are few and far between. Fortunately,  
127 the GNSS site infrastructure for deriving GNSS PWV is not nearly as demanding as for  
128 geodetic or plate tectonics studies. Highly non-ideal platforms such as flux towers (Adams  
129 et al. 2011a) or even moving oceanic vessels (Rocken et al. 2005; Kealy et al. 2012) can be  
130 utilized (see Sidebar).

131 The overarching motivation for the creation of the ADGMN was to address convection-  
132 humidity interactions, a major scientific challenge (Derbyshire et al. 2004; Kuang and Brether-  
133 ton 2006; Waite and Khouider 2010; Hohenegger and Stevens 2013). Convective parame-  
134 terizations are too insensitive to tropospheric humidity due to inadequate representation of  
135 entrainment of environmental air into convective updrafts (Kuang and Bretherton 2006; Ge-  
136 nio 2012). Entrainment in clouds remains a vital research question (Romps and Kuang 2010;  
137 Yeo and Romps 2013; Sherwood et al. 2013), and is a leading source of climate model uncer-  
138 tainty (Rougier et al. 2009). Furthermore, upscale growth and convective organization, also  
139 poorly represented with parameterized convection, are strongly linked to convective down-  
140 drafts/cold pools which, in turn, are sensitive to the vertical humidity structure (Tompkins  
141 2001a,b). A few convective parameterizations are beginning to address these effects (Rio  
142 et al. 2009; Mapes et al. 2009; Park 2014). Although neither entrainment nor the vertical  
143 humidity structure (however, see Section 6a) can be directly captured with GNSS dense  
144 meteorological networks, they can provide target relationships modified parameterization  
145 schemes must be able to replicate.

146 Diagnostic studies are needed to turn raw data into such model target results and suggest  
147 which physical processes are dominant (e.g., surface latent heat fluxes, horizontal advection,  
148 water vapor convergence, etc.) in the evolution of water vapor fields at these newly seen  
149 spatial and temporal resolutions. Adams et al. (2013) inferred using GNSS PWV from a

150 single station, a 4-hour water vapor convergence timescale indicative of the shallow-to-deep  
151 transition for the equatorial continental Tropics. With dense mesoscale networks, cross-  
152 correlations and other techniques will be able to identify the spatial/temporal scales of  
153 variability in PWV fields, putting mechanistic deductions on a firmer basis. Furthermore,  
154 PWV, in itself, is actually a much more valuable quantity than its integral nature might  
155 suggest (Holloway and Neelin 2009; Lintner et al. 2011). Empirical PWV/precipitation  
156 relationships are surprisingly strong (Zeng 1999; Bretherton et al. 2004) and theoretical  
157 views of tropical convection such as “self-organized criticality” (Neelin et al. 2009; Peters  
158 et al. 2009) or that of large-scale “thermodynamic control” (Raymond 2000) depend critically  
159 on PWV. These types of studies, all over oceanic regions, could be greatly expanded with  
160 GNSS meteorology and data over land may provide unique tests of such theories.

## 161 **4. Experimental Design, Instrumentation and Data**

162 The ADGMN consisted of two experiments: a 6-week campaign in and around Belem,  
163 which coincided with the CHUVA Belem campaign (Machado et al. 2014), and a one-year  
164 campaign in and around Manaus. As originally proposed (Adams et al. 2011b), the ADGMN  
165 was intended to coincide in Manaus with the CHUVA campaign in 2012. However, with the  
166 confirmation of the U.S. Department of Energy GOAmazon (Green Ocean Amazon) Cam-  
167 paign (see <http://campaign.arm.gov/goamazon2014/>), an elaborate experiment for exam-  
168 ining atmospheric chemistry, aerosols, cloud microphysics and convective precipitation in a  
169 tropical continental setting, CHUVA Manaus was postponed until 2014 when more instru-  
170 mentation was deployed. Nevertheless, constructing one phase of the ADGMN in Belem was  
171 fortuitous in that it was a successful demonstration of a dense GNSS meteorological network  
172 in a distinctive tropical convective regime driven by the sea breeze.

174 Convective development in the tropical sea-breeze regime has been studied in theoretical,  
175 modeling work and observationally in a wide variety of locales around the globe (Moncrieff  
176 and Liu 1999; Carbone et al. 2000; Mapes et al. 2003; Fovell 2005; Robinson et al. 2013).  
177 The sea breeze, driven by differential land/sea heating, orchestrates the timing and location  
178 of convective cell initiation (Moncrieff and Liu 1999; Fovell 2005; Robinson et al. 2013).  
179 However, once the convective cells begin to precipitate, cold pool/gust fronts and the envi-  
180 ronmental thermodynamical/shear conditions then determine whether upscale growth into  
181 propagating squall lines or mesoscale convective systems occur (Moncrieff and Liu 1999;  
182 Carbone et al. 2000). The Belem coastal region, unlike many previous tropical sea-breeze  
183 studies, such as Florida (Ulanski and Garstang 1978), is the coast of an enormous continen-  
184 tal region. The Belem area has two particularities: the striking punctuality <sup>1</sup> of the late  
185 afternoon convective activity (Kousky 1980; Angelis et al. 2004), and acting as the initiation  
186 point of spectacular, long-lived squall lines up to 2000 km in length penetrating, and even  
187 crossing, the Amazon Basin (Greco et al. 1990; Garstang et al. 1994; Cohen et al. 1995;  
188 Alcântara et al. 2011).

189 The Belem Dense GNSS Meteorological Network was initiated May 25th and dismantled  
190 July 7th. The network was composed of 15 GNSS/meteorological stations which provided  
191 high frequency (5 minutes) PWV as well as surface meteorological variables (Figure 1).  
192 Two nearly perpendicular transects were constructed: (1) southeast to northwest along the  
193 dominant lower-to-mid tropospheric east-southeasterly winds (BSMG-BSPC-BMSQ-BSOR  
194  $\sim 150$ km) and, (2) southwest to northeast, essentially perpendicular to the Atlantic coastline  
195 (BABT-BSSG  $\sim 100$ km). A cluster of stations, centered in Belem with approximately 10km  
196 separation distance were collocated with the CHUVA instrumentation array, described next.

197 The CHUVA project consisted of 6 field campaigns in different convective regimes in

---

<sup>1</sup>A common expression in Belem is “A gente se encontra antes ou depois da chuva?” (Should we meet before or after the rain?)

198 Brazil; including the sea-breeze regime of Belem and the continental tropical rainforest  
199 regime of Manaus. CHUVA was motivated by the need to better observe cloud microphysics  
200 in both warm and cold clouds and their associated precipitation processes in the Tropics  
201 (Calheiros and Machado 2014). The CHUVA Belem campaign included a suite of instru-  
202 mentation for documenting environmental thermodynamic conditions and cloud evolution  
203 and microphysics. Three radiosonde sites supplied thermodynamic stability variables, water  
204 vapor and wind profiles. A microwave radiometer furnished high frequency vertical water  
205 vapor structure and cloud liquid water profiles. An X-band dual polarization radar (X-Pol)  
206 was utilized to capture the development of convective clouds. Surface meteorological stations  
207 and disdrometers characterized rainfall intensity and hydrometeors, respectively. Twice-daily  
208 (8am and 8pm LT) radiosondes were launched (SBBE 82193, Belem Airport, near station  
209 BEMA) through the duration of the experiment. In addition, a 7-day intensive observational  
210 period included 4 extra launches per day (00:00, 06:00,12:00 and 18:00 UTC) in a triangu-  
211 lar arrangement with approximately 120 km separation distance between SBBE, São Miguel  
212 (BSMG) and further to the south at Tomé Açu ( $2.4167^\circ$  S,  $48.1500^\circ$  W), (not seen in Figure  
213 1). Details can be found in (Machado et al. 2014) and at <http://chuvaproject.cptec.inpe.br>.

214 *b. The Manaus Dense GNSS Meteorological Network*

215 The area around Manaus ( $2.61^\circ$  S,  $60.21^\circ$  W) (see Figure 2), in the central Amazon,  
216 in many respects is the quintessential continental tropical regime. Rainfall totals are large  
217 ( $\sim 2500\text{mm}\text{yr}^{-1}$ ) and distributed throughout the year, but with a notable dry season from  
218 July through September and the most frequent precipitation from January through April  
219 (Machado et al. 2004). Topographic variation across the network, from Amazon River sta-  
220 tions to forest stations is greater than Belem, but small nonetheless ( $\sim 150\text{m}$ ). It has been  
221 noted that these weak topographic gradients can induce local circulations with impacts on  
222 the precipitation distribution (Fitzjarrald et al. 2008; Betts et al. 2009). Typical of con-  
223 tinental tropical regimes, there is a strong afternoon peak in convective rainfall; however,

224 nocturnal events are not infrequent and travelling squall lines can arrive in or out of phase  
225 with diurnal surface heating (Greco et al. 1990; Angelis et al. 2004; Adams et al. 2013).

226 The Manaus network commenced in April 2011 with 12 GNSS meteorological stations.  
227 With the termination of the Belem campaign, the Manaus network expanded to 22 stations  
228 for the last 9 months (August 2011 to April 2012). Although the profiling instrumentation  
229 of CHUVA was not available, twice-daily radiosondes were launched from SBMN (see Figure  
230 2). In addition, the station at Embrapa (EMBP, green, north of Manaus), included a UV  
231 Raman Lidar (beginning September 2011) for frequent  $\sim 5$  minute nighttime water vapor  
232 profiles, as well as disdrometer and additional surface meteorological equipment. The station  
233 distribution can be categorized as low-lying river sites (CMP1, CHR5, CTLO, EMIR, HORT,  
234 MNCP, MNQI, PDAQ, TMB7), interior stations (CDN2, CDN4, GOAM, INPA, IRAN,  
235 JPL6, NAUS, PNT8) and forest-transition stations (EMBP, RDCK, RPDE, TRM3). Site  
236 ZF29 (blue, northern-most site), a rainforest GNSS site, was rather unconventional being  
237 located atop a 55m flux tower (K34) (see Figure 5) of the *Large Scale Biosphere/Atmosphere*  
238 *Experiment in Amazonia* (LBA), thereby offering an unprecedented look at rainforest PWV  
239 (Adams et al. 2011a). Although the network’s primary goal was to study the mesoscale  
240 evolution of convection, indirect measures of local circulations (e.g., between the Amazon  
241 River and surrounding forest) and their intensity can also be gauged. Furthermore, the  
242 network’s one-year duration means that the dry, wet and transition seasons were observed  
243 and seasonal effects on convective organization and PWV fields are available for analysis.

## 244 **5. Belem Results: The Diurnal Cycle of Sea-breeze Con-** 245 **vection**

246 For the 6 week duration of the Belem experiment, days were categorized as “convective”  
247 (22 days) or “non-convective” (19 days), based solely on a minimum cloud top temperature  
248 of 240K or below over the central portion of the network and a report of precipitation at

249 at least one site during the afternoon or evening. Composites of the temporal evolution  
250 of PWV and cloud top temperature are shown in Figure 3. To gauge the environmental  
251 conditions in which convection developed (or not), average thermodynamic stability (CAPE  
252 and CIN), water vapor profiles and wind shear magnitude were calculated. The Belem  
253 network lacks any significant variations in topography along the coast and bay and boundary  
254 layer thermodynamics are also quite uniform. During the intensive observational period, the  
255 standard deviation of mixing ratio and temperature averaged over the lowest 50hPa in all  
256 soundings from all 3 sites and all launch times, were  $1.1gkg^{-1}$  and  $1.0^{\circ}C$ , respectively. The  
257 reasons for convective development on any given day are quite subtle.

258 The composites of GNSS PWV and cloud top temperature for 3 stations (BSSG, BBNV  
259 and BABT), aligned SW/NE almost perpendicularly to the broadscale coastline and ad-  
260 vancing sea-breeze lines, are shown in Figure 3. Morning values of PWV and cloud top  
261 temperature are similar for convective and non-convective days, but differences begin to  
262 appear about 10am.  $\frac{\Delta PWV}{\Delta t}$ , mostly a measure of water vapor convergence (Adams et al.  
263 2013), was estimated between the upward and downward pointing triangles for each site in  
264 Figure 3. The propagation speed of the convective perturbation between BSSG/BBNV and  
265 BBNV/BABT was calculated by dividing between-station distance by the time difference  
266 between maximum PWV at each site (upward pointing triangles). These two propagation  
267 speeds were then averaged.  $\frac{\Delta PWV}{\Delta t}$  is more than 50% greater for convective days and the  
268 convective propagation speed is nearly twice as large (see Table 1).

269 What promotes or inhibits the development and propagation of convection in Belem’s sea-  
270 breeze regime? In addition to propagation speed and water vapor convergence, environmental  
271 conditions, including moist stability as measured by CAPE/CIN, the windshear magnitude  
272 between the steering level and near-surface layer (Carbone et al. (2000)) and water vapor,  
273 both near surface and from 850 to 500hPa were calculated from the 8am LT soundings  
274 (Table 1). The vertical water vapor distribution and wind shear magnitude (and direction,  
275 not shown) are essentially the same for both convective and non-convective days. However,

276 morning CAPE is twice as large on convective days. Nevertheless, a  $1gkg^{-1}$  and  $1^{\circ}C$  increase  
277 in surface mixing ratio and temperature; that is, the observed standard deviations, would  
278 increase CAPE by more than  $1000Jkg^{-1}$ , larger than the convective-nonconvective difference  
279 of  $500Jkg^{-1}$ . Although the number of cases is small, it would be difficult to argue that deep  
280 convection or its suppression are solely functions of environmental instability, wind-shear  
281 and water vapor structure.

282 Convective growth or suppression appears to be closely tied to the morning formation  
283 of convective lines within 30km or so of the coast (presumably along the sea-breeze front).  
284 Time loops of GOES 12 IR imagery over a much larger region than the Belem network  
285 support this contention. Figure 3 shows the average cloud top temperature at 12:30pm local  
286 time for convective and non-convective days. Convective days begin with the formation, by  
287 10am, of near coastal cumulus cells. By noon, cumulus congestus develop above the freezing  
288 level, begin to coalesce and commence propagating inland. In contrast, for non-convective  
289 days, cumulus cells develop later in the morning, remain closer to the coast and only weakly  
290 coalesce, quickly dissipating before propagating further inland (See Supplemental Material  
291 (Caption: Animations of 15 minutes GOES 12 IR imagery over the northern Brazilian coast  
292 near Belem for Convective days (Left) and Non-convective days (right))). These impressions  
293 suggest a prominent role for gust fronts and cold pools and secondary development in the  
294 organization and propagation of these convective lines. What promotes the initial convective  
295 formation along the coast in the first place? Subtle changes in interactions between the sea-  
296 breeze front and synoptic-scale flow patterns may be at play, similar to seasonal variability  
297 in large-scale flow over the region (Kousky 1980).

#### 298 *a. Future Belem Network Studies*

299 Given the soundings, surface meteorological and cloud microphysical data gathered by  
300 CHUVA and the ADGMN, the role of advancing cold pools/gust fronts forcing convection  
301 can be surmised in future work. Our portrait of the evolution of Belem sea-breeze con-

vection presented in the previous section, although a bit speculative, is entirely consistent with a quiescent large-scale, but mildly thermodynamically unstable, environment where premoistening of the free troposphere to support deep convection is not required. Here, propagating cold pools provide the necessary kick for releasing convective instability leading to cloud growth and precipitation and further propagation. With the existing dense network and CHUVA data set, dynamic lifting provided by cold pools/gust fronts can be examined directly through cloud spatial/temporal evolution (X-pol radar) and visible and IR cloud fields (GOES 12 satellite). Surface meteorological stations will provide temperature drops and wind gusts for cold pool/gust front identification and, finally, GNSS stations will furnish  $\frac{\Delta PWV}{\Delta t}$  at each station along the convective line trajectory. Adams et al. (2013) hypothesized, during the transition to deep convection and prior to heavy precipitation, cloud condensate formation and advection and surface evaporation are secondary in the total column water conservation budget. These ideas can be put to the test with the Belem data set. Furthermore, given the homogeneity in Belem low-level water vapor fields, horizontal advection is weak, and thus GNSS  $\frac{d(PWV)}{dt}$  represents vertical water vapor advection, providing a window into vertical motion, which is very difficult to measure directly.

## 6. Manaus Results: Seasonal and Topographic Effects on the Diurnal Cycle

In light of the longer-term deployment of stations in and around Manaus, studies involving the seasonal influences on convection and topographically forced mesoscale circulation can also be addressed. Local topography and vegetated surfaces, perturbed and unperturbed, can induce mesoscale circulations along the Amazon River which influence cloud and precipitation distributions (Silva-Dias et al. 2004; Fitzjarrald et al. 2008). Local circulations driven by anthropogenic deforestation have especially received attention (Wang et al. 2009; Saad et al. 2010). Local mesoscale breezes can enhance cloud formation over vegetated zones,

327 while suppressing it over the river due to subsidence. Enhanced cloud formation should be  
328 associated with increases in precipitation for typical diurnal cycle convection, all else being  
329 equal. Fitzjarrald et al. (2008) found that near-river sites do receive less afternoon rainfall  
330 as expected, but their nocturnal rainfall can be enhanced due to interactions with squall  
331 lines and local river geometry.

332 From the year of Manaus network data, Figure 4 presents the PWV diurnal cycle as a  
333 function of location and season. The diurnal cycle of PWV was calculated at an interior,  
334 forest and two river sites for the dry, dry-to-wet transition and wet season, the results of  
335 which can be seen in Figure 4. Based solely on the forest/river contrast, which is difficult to  
336 separate from the topographical effect, it is apparent that the forested site ZF29 experiences a  
337 more robust diurnal cycle, particularly when compared with CHR5, a river site. The seasonal  
338 effect on the PWV diurnal cycle is principally that water vapor convergence is earlier in the  
339 day (true for all sites) and generally less intense during the wet season. The dry season  
340 and dry-to-wet transition seasons have larger amplitude diurnal rises for both the interior  
341 site, JPL6, and ZF29. This is not true, however, for CHR5 where the dry season diurnal  
342 cycle is strongly muted. The behavior of all of the river sites is not consistent and appears  
343 to be strongly influenced by their very local setting with respect to the dominant lower  
344 tropospheric easterly winds and the Manaus “peninsula” (See Figure 2). For comparison  
345 purposes, an “upwind” river site (HORT) is also included in Figure 4. The diurnal cycle  
346 at HORT is much more pronounced than CHR5, mimicking other interior stations. The  
347 other river stations on the “downwind” side of the Manaus peninsula (CMP1, TMB7) share  
348 this seasonal behavior with CHR5. Recalling that  $\frac{\Delta PWV}{\Delta t}$  is a glimpse of vertical motion,  
349 these results offer strong evidence that local topographic effects do indeed induce mesoscale  
350 circulations. How these local convergence patterns affect the development of convection  
351 still remains to be investigated. But, these results indicate that GNSS meteorology may  
352 also be an incisive test for model-generated mesoscale circulations, even for non-convective  
353 conditions.

355 The Manaus network lends itself to the study of cumulus congestus cold pools and their  
356 role in the shallow-to-deep transition to deep precipitating cumulonimbus cells and their  
357 organization on the mesoscale. Numerical modeling work by Khairoutdinov and Randall  
358 (2006), based on Amazonian-inspired boundary conditions, identifies the space and time  
359 scales that are associated with congestus cold pool formation, convergence and the shallow-  
360 to-deep transition. The density of stations in the central portion of the network is more than  
361 adequate to capture cold pool formation. Cold pools and convective downdrafts can be iden-  
362 tified via surface stations, while PWV fields will indicate water vapor convergence/advection.  
363 Meanwhile, GOES 12 visible and IR document the growth, organization and propagation of  
364 cumulus into cumulonimbus lines/clusters. The frequent convective events over the Manaus  
365 network should furnish sufficient cases to ascertain the role of cold pools in the shallow-to-  
366 deep convective transition.

367 One exciting prospect is that with a dense network of GNSS receivers, 3D water vapor  
368 structure may be possible to retrieve (Braun et al. 2001; Bastin et al. 2007; Champollion  
369 et al. 2009). Tropospheric tomography divides the earth’s atmosphere into small volume  
370 elements or “voxels” and uses the slant delays (between the satellite and the receiver) to  
371 estimate the refractivity in each voxel and, hence, a vertical profile of refractivity. This  
372 refractivity can be transformed through algebraic iterative techniques into 3D water vapor  
373 estimates (Bender et al. 2011). This tomographic software is currently being developed at  
374 the Departamento de Informática, Universidade da Beira Interior, Covilhã, Portugal. The  
375 ADGMN, both Belem and Manaus, are ideal for developing such 3D estimates given the  
376 available soundings for constraining and validating the technique.

## 7. GNSS Networks in the Tropics

Though mesoscale meteorological GNSS networks are absent in the Tropics, larger scale networks have been (Bock et al. 2008) and are presently being constructed. The CONet project (Braun et al. 2012) is constructing 139 GNSS meteorology sites for studying Caribbean climate and meteorology and tectonic activity in the region. These permanent real-time PWV stations (101 of which are currently online), scattered across the Caribbean, can serve as anchor sites for the development of both long-term and campaign mesoscale dense networks to study convection and water vapor fields in the tropical tradewind regime. Another promising development in the Tropics was the joint U.S./Mexico *North American Monsoon GNSS Transect Experiment 2013*, a mesoscale meteorological transect across the complex terrain of the Sierra Madre Occidental in northwest Mexico (Adams et al. 2014). Across the rest of Mexico, TlalocNet (<http://www.unavco.org/projects/major-projects/tlalocnet/tlalocnet.html>) aims to develop a large-scale geodetic and atmospheric infrastructure for geoscience studies. 18 new real-time GNSS meteorology sites, including a permanent extension of the *North American Monsoon GNSS Transect Experiment 2013* are being installed. Dense Networks anchored to these Mexican and Caribbean sites would offer a wide variety of topographic settings and meteorological regimes to complement sea-breeze and continental tropical data from Brazil described above.

Since unstable oceanic platforms can even be employed, the expansion of GNSS meteorology into viable tropical oceanic regions should be promoted over ocean, local surface evaporation is a small contributor to PWV and well-measured, strengthening the interpretation of  $dPWV/dt$  as representative of vertical motion (Yasunaga et al. 2008). Finally, for the long term, the precision of GNSS-derived PWV will increase as more satellites come online in addition to GPS (e.g. GLONASS, Galileo and Beidou), increasing the value of this stable platform for observing global climate variability.

403 As noted, the spread of GNSS meteorology into logistically difficult regions such as the  
404 Amazon requires compromises when it comes to GNSS installations. Geodetic requirements  
405 for antenna permanence, such as rigid monumentation, full-sky visibility, and absence of  
406 obstructions can be relaxed for GNSS meteorological applications without serious deterio-  
407 ration of the data collected. Even in the extreme case of installing a GNSS antenna on  
408 scaffolding above the forest canopy, useful data can still be collected if the motions of the  
409 scaffold were constrained to minimize vertical displacements of the antenna phase center  
410 over time. Relaxing these requirements also reduces the financial burden on the campaign,  
411 since local/indigenous resources can be exploited to accomplish the experimental objectives.  
412 For the Amazon Dense Network campaign sites, perfectly valid PWV values were captured  
413 from a 55 meter INPA/LBA Flux tower (ZF29), a chicken coop (HORT), housing on stilts  
414 “palafitas” suffering annual flooding (CTLO) and residential housing (BJRN) (see Figure  
415 5). For permanent sites which serve both the Geodesy/Geophysics and the meteorology  
416 community, more stringent conditions exist and, clearly, these sites would not be adequate  
417 for measuring the necessary millimeter displacements in position.

418 For meteorological campaigns (longer than several weeks), the lack of need for stable  
419 monumentation drastically lowers installation costs. A geodetic grade receiver/antenna and  
420 a surface meteorological station (with real time capacity were internet available) is now less  
421 than 10,000 dollars (in the U.S.) for a meteorological campaign-ready installation. These  
422 receivers/antennas are extremely robust and durable and serve as a datalogger with greater  
423 than one year capacity for data storage at the typical data collection rate required. Energy  
424 requirements are small ( $\sim 4W$ ) so solar panels and deep cycle batteries can be employed,  
425 although maintenance costs for deep cycle batteries depend on climatic regime. Given the  
426 frequent power outages in the Amazon and lack of solar panels for the the ADGMN, both  
427 Belem and Manaus, a workable energy set up consisted of a trickle charger plugged in to  
428 local current and two car batteries in parallel giving at least two days of independent power.

429 The entire process of installation, maintenance and data collection is relatively straight-  
430 forward. Students from the graduate program *Clima e Ambiente* from the Universidade  
431 do Estado do Amazonas in Manaus participated in the installation of both the Belem and  
432 Manaus networks as well as the maintenance and data collection from these sites.

433 *Acknowledgments.*

434 We would like to thank Dr. Antônio Manzi, Hilândia Cunha e Cícero Leite of the  
435 INPA/LBA for financial, logistical and technical support for this project. Special thanks  
436 also go to Lúcia Soares de Oliveira, Edson Ferreira de Assunção, Carlos Vicente Ferreira,  
437 Francisco Paulo Santos, Prefeito of Manaquiri, Fundação Amazonas Sustentável Tumbira,  
438 Embrapa, and Reserva Ducke for hosting stations. We also thank Earle Williams and David  
439 Fitzjarrald for their comments on the original manuscript. Likewise, Brian Mapes greatly  
440 helped with the manuscript and the IDV animations. Figures were made with NCL. Sup-  
441 port for this project and the Amazonian Dense GNSS Meteorological Network comes through  
442 cooperation project 0050.0045370.08.4 between PETROBRAS and INPE (Brazil) (Icaro Vi-  
443 torello, Principal Investigator) and SMOG (PTDC/CTEATM/119922/2010) funded by FCT  
444 (Portugal). The CHUVA Project was funded by FAPESP grant No. 2009/15235-8. Also, we  
445 would like to thank UNAVCO's Equipment Loan Program for providing GPS receivers for  
446 the Belem Network. The ADGMN was carried out while the first author was faculty in the  
447 Programa de Pós Graduação em Clima e Ambiente, Universidade do Estado do Amazonas,  
448 Manaus, Amazonas, Brazil.

## REFERENCES

- 451 Adams, D. K., R. M. S. Fernandes, and J. M. F. Maia, 2011a: GNSS Precipitable Water  
452 Vapor from an Amazonian Rain Forest Flux Tower. *Journal of Atmospheric and Oceanic*  
453 *Technology*, **28**, 1192–1198.
- 454 Adams, D. K., S. I. Gutman, K. L. Holub, and D. S. Pereira, 2013: GNSS observations of  
455 deep convective time scales in the Amazon. *Geophys. Res. Lett.*, **40**, 2818–2823.
- 456 Adams, D. K., C. Minjarez, Y. Serra, A. Quintanar, L. Alatorre, A. Granados, E. Vázquez,  
457 and J. Braun, 2014: Mexican GPS tracks convection from North American Monsoon.  
458 *EOS. Transactions of the American Geophysical Union*, **95 (7)**, 61–68.
- 459 Adams, D. K., et al., 2011b: A Dense GNSS Meteorological network for observing deep  
460 convection in the Amazon. *Atmos. Sci. Lett.*, **12**, 207–212, doi:10.1002/asl.312.
- 461 Alcântara, C. R., M. A. F. Silva-Dias, E. P. Souza, and J. C. P. Cohen, 2011: Verification of  
462 the role of the low level jets in Amazon squall lines. *Atmospheric Research*, **100**, 36–44.
- 463 Angelis, C. F., G. R. McGregor, and C. Kidd, 2004: Diurnal cycle of rainfall over the  
464 Brazilian Amazon. *Climate Research*, **26**, 139–149.
- 465 Bastin, S., C. Champollion, O. Bock, P. Drobinski, and F. Masson, 2007: Diurnal cycle of  
466 water vapor as documented by a dense GPS network in a coastal area during ESCOMPTE  
467 IOP2. *Journal of Applied Meteorology and Climatology*, **46**, 167–182.
- 468 Bechtold, P., J. Chaboureau, A. Beljaars, A. Betts, M. Kohler, M. Miller, and J. Re-  
469 delsperger, 2004: The simulation of the diurnal cycle of convective precipitation over  
470 land in a global model. *Quart. J. Roy. Meteor. Soc.*, **130**, 3119–3137.

471 Bender, M., G. Dick, M. Ge, Z. Deng, J. Wickert, H.-G. Kahle, A. Raabe, and G. Tetzlaff,  
472 2011: Development of a gnss water vapor tomography system using algebraic reconstruc-  
473 tion technique. *Advances in Space Research*, **47**, 1704–1720.

474 Betts, A. K., G. Fisch, C. von Randow, M. A. F. Silva-Dias, J. C. P. Cohen, R. da Silva, and  
475 D. R. Fitzjarrald, 2009: The Amazonian boundary layer and mesoscale circulations. *Ama-  
476 zonia and Global Change*, American Geophysical Union, No. 186 in Geophysical Mono-  
477 graph Series, 163 – 181.

478 Betts, A. K. and C. Jakob, 2002a: Evaluation of the diurnal cycle of precipitation, surface  
479 thermodynamics, and surface fluxes in the ECMWF model using LBA data. *J. Geophys  
480 Res.*, **107**, doi:10.1029/2001JD000427.

481 Betts, A. K. and C. Jakob, 2002b: Study of diurnal convective precipitation over Amazonia  
482 using a single column model. *J. Geophys Res.*, **107**, doi:10.1029/2001JD002264.

483 Bevis, M., S. Businger, T. A. Herring, C. Rocken, R. Anthes, and R. H. Ware, 1992: GPS  
484 meteorology: Sensing of atmospheric water vapor using the Global Positioning System. *J.  
485 Geophys Res.*, **97**, 15 787–15 801.

486 Bock, O., et al., 2008: West African Monsoon observed with ground-based GPS receivers  
487 during African Monsoon Multidisciplinary analysis (AMMA). *J. Geophys Res.*, **113**, doi:  
488 10.1029/2008JD010327.

489 Braun, J., C. Rocken, and R. Ware, 2001: Validation of line-of-site water vapor measure-  
490 ments with GPS. *Radio Science*, **36**, 459–472.

491 Braun, J. J., G. Mattioli, D. C. E. Calais, M. Jackson, R. Kursinski, M. Miller, and  
492 R. Pandya, 2012: Multi-disciplinary natural hazards research initiative begins across  
493 Caribbean basin. *EOS. Transactions of the American Geophysical Union*, **93**, doi:  
494 10.1029/2012EO090001.

495 Brenot, H., et al., 2013: Preliminary signs of the initiation of deep convection by GNSS.  
496 *Atmos. Chem. Phys.*, **13**, 5425–5449, doi:10.5194/acp-13-5425-2013.

497 Bretherton, C. S., M. E. Peters, and L. E. Back, 2004: Relationships between water vapor  
498 path and precipitation over the tropical oceans. *Journal of Climate*, **17**, 1517–1528.

499 Calheiros, A. and L. Machado, 2014: Cloud and rain liquid water statistics in the CHUVA  
500 campaign. *Atmospheric Research*, **144**, 126–140.

501 Carbone, R. E., J. W. Wilson, T. D. Keenan, and J. M. Hacker, 2000: Tropical island  
502 convection in the absence of significant topography. Part I: Life cycle of diurnally forced  
503 convection. *Monthly Weather Review*, **128**, 3459–3480.

504 Champollion, C., C. Flamant, O. Bock, F. Masson, D. D. Turner, and T. Weckwerth, 2009:  
505 Mesoscale GPS tomography applied to the 12 June 2002 convective initiation event of  
506 IHOP\_2002. *Quart. J. Roy. Meteor. Soc.*, **135**, 645–662.

507 Champollion, C., F. Masson, M.-N. Bouin, A. Walpersdorf, E. Doerflinger, O. Bock, and  
508 J. van Baelen, 2005: GPS water vapor tomography: Preliminary results from the ES-  
509 COMPTE field experiment. *Atmos. Res.*, **74**, 253–274.

510 Cohen, J. P., M. A. F. Silva-Dias, and C. A. Nobre, 1995: Environmental conditions associ-  
511 ated with Amazonian squall lines: A case study. *Mon. Wea. Rev.*, **123**, 3163–3174.

512 Derbyshire, S. H., I. Beau, P. Bechtold, J.-Y. Grandpeix, J. Piriou, J.-L. Redelsperger, and  
513 P. M. M. Soares, 2004: Sensitivity of moist convection to environmental humidity. *Quart.*  
514 *J. Roy. Meteor. Soc.*, **130**, 3055–3079.

515 Duan, J., et al., 1996: GPS meteorology: Direct estimation of the absolute value of precip-  
516 itable water. *J. Appl. Meteor.*, **35**, 830–838.

517 Fitzjarrald, D. R., R. K. Sakai, O. L. L. Moraes, R. C. de Oliveira, O. C. Acevedo,

- 518 M. J. Czikowsky, and T. Beldini, 2008: Spatial and temporal rainfall variability near  
519 the Amazon-Tapajós confluence. *J. Geophys Res.*, **113**, doi:10.1029/2007JG000596.
- 520 Fovell, R. G., 2005: Convective initiation ahead of the sea-breeze front. *Mon. Wea. Rev.*,  
521 **133**, 264–278.
- 522 Garstang, M., H. L. M. JR., J. Halverson, S. Greco, and J. Scala, 1994: Amazon coastal  
523 squall lines. part I: Structure and kinematics. *Mon. Wea. Rev.*, **122**, 608–622.
- 524 Garstang, M., et al., 1990: The Amazon Boundary-Layer Experiment (ABLE 2B): A Mete-  
525 orological Perspective. *Bull. Amer. Meteor. Soc.*, **91**, 19–32.
- 526 Genio, A. D. D., 2012: Representing the sensitivity of convective cloud systems to tropo-  
527 spheric humidity in general circulation models. *Survey of Geophysics*, **33**, 637–656.
- 528 Grabowski, W. W. and M. W. Moncrieff, 2004: Moisture-convection feedback in the tropics.  
529 *Quart. J. Roy. Meteor. Soc.*, **130**, 3081–3104.
- 530 Grabowski, W. W., et al., 2006: Daytime convective development over land: A model  
531 intercomparison based on LBA observations. *Quart. J. Roy. Meteor. Soc.*, **132**, 317–344.
- 532 Greco, S., et al., 1990: Rainfall and surface kinematic conditions over central Amazonia  
533 during ABLE 2B. *J. Geophys. Res.*, **95**, 17 001–17 014.
- 534 Hohenegger, C. and B. Stevens, 2013: Preconditioning deep convection with cumulus con-  
535 vection. *J. Atmos. Sci.*, **70**, 448–464.
- 536 Holloway, C. E. and J. D. Neelin, 2009: Moisture vertical structure, column water vapor,  
537 and tropical deep convection. *J. Atmos. Sci.*, **66 (6)**, 1665–1683.
- 538 Kealy, J., J. Foster, and S. Businger, 2012: GPS meteorology: An investigation of ocean-  
539 based precipitable water estimates. *J. Geophys Res.*, **117**, doi:10.1029/2011JD017422.

540 Khairoutdinov, M. and D. Randall, 2006: High-resolution simulation of shallow-to-deep  
541 convection transition over land. *J. Atmos. Sci.*, **63**, 3421–3436.

542 Kousky, V., 1980: Diurnal rainfall variation in Northeast Brazil. *Mon. Wea. Rev.*, **108**,  
543 488–498.

544 Kuang, Z. and C. S. Bretherton, 2006: A mass-flux scheme view of a high-resolution sim-  
545 ulation of a transition from shallow to deep cumulus convection. *J. Atmos. Sci.*, **63**,  
546 1895–1909.

547 Kursinski, E. R., G. A. Hajj, S. Leroy, and B. Herman, 2000: The GPS radio occultation  
548 technique. *Terrestrial, Atmospheric and Oceanic Sciences*, **11**, 53–114.

549 Kursinski, E. R., et al., 2008: Water vapor and surface observations in northwestern Mexico  
550 during the 2004 NAME enhanced observing period. *Geophys. Res. Lett.*, **35**, doi:10.1029/  
551 2007GL031404.

552 Lintner, B. R., C. E. Holloway, and J. D. Neelin, 2011: Column water vapor statistics and  
553 their relationship to deep convection, vertical and horizontal circulation, and moisture  
554 structure at Nauru. *J. Climate*, **24**, 5454–5466.

555 Machado, L. A. T., H. Laurent, N. Dessay, and I. Miranda, 2004: Seasonal and diurnal  
556 variability of convection over the Amazonia: A comparison of different vegetation types  
557 and large scale forcing. *Theor. Appl. Climatol.*, **78**, 61–77, doi:0.1007/s00704-004-0044-9.

558 Machado, L. A. T., et al., 2014: The CHUVA Project-How does convection vary across  
559 Brazil? *Bulletin of the American Meteorological Society*, **95**, 1365–1380.

560 Mapes, B., R. Milliff, and J. Morzel, 2009: Composite life cycle of maritime tropical  
561 mesoscale convective systems in scatterometer and microwave satellite observations. *J.*  
562 *Atmos. Sci.*, **66**, 199–208.

- 563 Mapes, B. and R. Neale, 2011: Parameterizing convective organization to escape the en-  
564 trainment dilemma. *J. Adv. Model. Earth Syst.*, **3**(2).
- 565 Mapes, B., T. Warner, and M. Xu, 2003: Diurnal patterns of rainfall in northwestern South  
566 America. Part III: Diurnal gravity waves and nocturnal convection offshore. *Mon. Wea.*  
567 *Rev.*, **131**, 830–844.
- 568 Masunaga, H., 2013: A satellite study of tropical moist convection and environmental vari-  
569 ability. *J. Atmos. Sci.*, **70**, 2443–2466.
- 570 Mazany, R. A., S. Businger, S. I. Gutman, and W. Roeder, 2002: A lightning prediction index  
571 that utilizes GPS integrated precipitable water vapor. *Wea. Forecasting*, **17**, 1034–1047.
- 572 Moncrieff, M. W. and C. Liu, 1999: Convective initiation by density currents: Role of  
573 convergence, shear and dynamical organization. *Mon. Wea. Rev.*, **127**, 2455–2464.
- 574 Moncrieff, M. W., D. E. Waliser, M. J. Miller, M. A. Shapiro, G. R. Asrar, and J. Caughey,  
575 2012: Multiscale convective organization and the YOTC Virtual Global Field Campaign.  
576 *Bull. Amer. Meteor. Soc.*, **93**, 1171–1187.
- 577 Neelin, J. D., O. Peters, and K. Hales, 2009: The transition to strong convection. *J. Atmos.*  
578 *Sci.*, **66**, 2367–2384.
- 579 Park, S., 2014: Unified Convection Scheme, UNICON. Part I. Formulation. *J. Atmos. Sci.*,  
580 **71**, 3902–3930.
- 581 Peters, O., J. D. Neelin, and S. W. Nesbitt, 2009: Mesoscale convective systems and critical  
582 clusters. *J. Atmos. Sci.*, **66**, 2913–2924.
- 583 Raymond, D. J., 2000: Thermodynamic control of tropical rainfall. *Quart. J. Roy. Meteor.*  
584 *Soc.*, **126**, 889–898.

585 Rio, C., F. Hourdin, J.-Y. Grandpeix, and J.-P. Lafore, 2009: Shifting the diurnal cy-  
586 cle of parameterized deep convection over land. *Geophys. Res. Lett.*, **36**, doi:10.1029/  
587 2008GL036779.

588 Robinson, F. J., M. D. Patterson, and S. C. Sherwood, 2013: A numerical modeling study  
589 of the propagation of idealized sea-breeze density currents. *J. Atmos. Sci.*, **70**, 653–668.

590 Rocken, C., J. Johnson, T. V. Hove, and T. Iwabuchi, 2005: Atmospheric water vapor and  
591 geoid measurements in the open ocean with GPS. *Geophys. Res. Lett.*, **32**, doi:10.1029/  
592 2005GL022573.

593 Rocken, C., R. H. Ware, T. V. Hove, F. Solheim, C. Alber, J. Johnson, M. Bevis, and  
594 S. Businger, 1993: Sensing atmospheric water vapor with the Global Positioning System.  
595 *Geophys. Res. Lett.*, **20**, 2631–2634.

596 Romps, D. M. and Z. M. Kuang, 2010: Do undiluted convective plumes exist in the upper  
597 tropical troposphere? *J. Atmos. Sci.*, **67**, 468–484.

598 Rougier, J., D. M. H. Sexton, J. M. Murphy, and D. Stainforth, 2009: Analyzing the cli-  
599 mate sensitivity of the HadSM3 climate model using ensembles from different but related  
600 experiments. *J. Climate*, **22**, 3540–3557.

601 Saad, S. I., H. R. da Rocha, M. A. F. Silva-Dias, and R. Rosolem, 2010: Can the deforestation  
602 breeze change the rainfall in Amazonia? A case study for the BR-163 highway region. *Earth*  
603 *Interactions*, **14**, 1–25.

604 Sapucci, L. F., L. A. T. Machado, J. F. G. Monico, and A. Plana-Fattori, 2007: Intercom-  
605 parison of integrated water vapor estimates from multisensors in the Amazonian region.  
606 *Journal of Atmospheric and Oceanic Technology*, **24**, 1880–1894.

607 Schlemmer, L. and C. Hohenegger, 2014: The formation of wider and deeper clouds as a  
608 result of cold-pool dynamics. *J. Atmos. Sci.*, **71**, 2842–2858.

609 Seko, H., H. Nakamura, Y. Shoji, and T. Iwabuchi, 2004: The Meso- $\gamma$  scale water vapor  
610 distribution associated with a thunderstorm calculated from a dense network of GPS  
611 receivers. *Journal of the Meteorological Society of Japan*, **82**, doi:10.1029/2005GL022573.

612 Sherwood, S., R. Roca, T. Weckwerth, and N. Andronova, 2009: Tropospheric water vapor,  
613 convection and climate: a critical review. *Rev. Geophys.*, **48**, doi:10.1029/2009RG000301.

614 Sherwood, S. and R. Warhlich, 1999: Observed evolution of tropical deep convective events  
615 and their environment. *Mon. Wea. Rev.*, **127**, 1777–1795.

616 Sherwood, S. C., D. Hernandez-Decker, and M. Colin, 2013: Slippery thermals and the  
617 cumulus entrainment paradox. *J. Atmos. Sci.*, **70**, 2426–2442.

618 Silva-Dias, M. A. F., P. L. Silva-Dias, M. Longo, D. R. Fitzjarrald, and A. S. Denning, 2004:  
619 River breeze circulation in eastern Amazonia: observations and modelling results. *Theor.*  
620 *Appl. Climatol.*, **78**, doi:10.1007/s00704-004-0047-6.

621 Silva-Dias, M. A. F., et al., 2002: Cloud and rain processes in a biosphere atmosphere inter-  
622 action context in the Amazon region. *J. Geophys Res.*, **107**, doi:10.1029/2001JD000335.

623 Tompkins, A., 2001a: Organization of tropical convection in low vertical wind shears: The  
624 role of cold pools. *J. Atmos. Sci.*, **58**, 1650–1672.

625 Tompkins, A., 2001b: Organization of tropical convection in low vertical wind shears: The  
626 role of water vapor. *J. Atmos. Sci.*, **58**, 529–545.

627 Ulanski, S. and M. Garstang, 1978: The role of surface divergence and vorticity in the life  
628 cycle of convective rainfall. part i: Observation and analysis. *J. Atmos. Sci.*, **35**, 1047–  
629 1062.

630 Waite, M. L. and B. Khouider, 2010: The deepening of tropical convection by congestus  
631 preconditioning. *J. Atmos. Sci.*, **67**, 2601–2615.

- 632 Wang, J., et al., 2009: Impact of deforestation in the Amazon basin on cloud climatology.  
633 *Proc. Nat. Acad. Sci.*, **106**, 3670–3674.
- 634 Wolfe, D. E. and S. I. Gutman, 2000: Developing an operational, surface-based, GPS, water  
635 vapor observing system for NOAA: Network design and results. *Journal of Atmospheric  
636 and Oceanic Technology*, **17**, 426–440.
- 637 Wu, C.-M., B. Stevens, and A. Arakawa, 2009: What controls the transition from shallow  
638 to deep convection? *J. Atmos. Sci.*, **66**, 1793–1806.
- 639 Yasunaga, K., M. Fujita, T. Ushiyama, K. Yoneyama, Y. N. Takayabu, and M. Yoshizaki,  
640 2008: Diurnal variations in precipitable water observed by shipborne GPS over the tropical  
641 Indian Ocean. *SOLA*, **4**, 97–100.
- 642 Yeo, K. and D. M. Romps, 2013: Measurement of convective entrainment using Lagrangian  
643 particles. *J. Atmos. Sci.*, **70**, 266–277.
- 644 Zeng, X., 1999: The relationship among precipitation, cloud-top temperature, and precip-  
645 itable water over the tropics. *Journal of Climate*, **12**, 2503–2514.
- 646 Zhang, C., J. Gottschalck, E. D. Maloney, M. Moncrieff, F. Vitart, D. E. Waliser, B. Wang,  
647 and M. C. Wheeler, 2013: Cracking the MJO nut. *Geophys. Res. Lett.*, doi:0.1002/grl.  
648 50244.

649 **List of Tables**

650 1 Thermodynamic and Dynamic Characteristics for the 22 Convective and 19  
651 Non-Convective days. CAPE, CIN, PWV, PWV(850-500mb) and Shear were  
652 calculated from the 8am (12Z) soundings.  $\frac{\Delta PWV}{\Delta t}$  representing “water vapor  
653 convergence” and Propagation Speed were calculated from the GNSS sites  
654 used in Figure 3.

27

TABLE 1. Thermodynamic and Dynamic Characteristics for the 22 Convective and 19 Non-Convective days. CAPE, CIN, PWV, PWV(850-500mb) and Shear were calculated from the 8am (12Z) soundings.  $\frac{\Delta PWV}{\Delta t}$  representing “water vapor convergence” and Propagation Speed were calculated from the GNSS sites used in Figure 3.

	CAPE $\text{Jkg}^{-1}$	CIN $\text{Jkg}^{-1}$	PWV cm	PWV 850 to 500mb cm	$\frac{\Delta PWV}{\Delta t}$ $\text{cmhr}^{-1}$	Propagation Speed. $\text{ms}^{-1}$	Shear $10^{-3}\text{s}^{-1}$
Convective (22 days)	1121.0	2.44	4.35	1.74	0.094	10.9	2.2
Non Convective (19 days)	549.0	3.32	4.23	1.77	0.064	5.8	1.9

## 655 List of Figures

- 656 1 Map of the Belem Dense GNSS Meteorological Network during the CHUVA  
657 experiment June 2011. Sounding sites were BSMG and BSSE (near BEMA).  
658 Tomé Açú is to the south of the mapped region. The large water body west  
659 of Belem is the Bahia de Marajó. 29
- 660 2 Map of the Manaus Dense GNSS Meteorological Network, April 2011 - April  
661 2012. Green and blue stations were present for the duration of the experiment.  
662 Red stations were present from August 2011 to April 2012. SBMN (82332)  
663 is the site for twice daily radiosondes and represents the tip of the Manaus  
664 “peninsula”. 30
- 665 3 Plot of timeseries of average PWV (every 5 minutes) BSSG (black,short dash),  
666 BBNV(red, long dash) and BABT(blue, solid) and average cloud top temper-  
667 ature (CTT) (every 15 minutes) (Identical patterns and colors, but thinner  
668 lines) for convective days (N =22) (upper left-hand plot) and non-convective  
669 days (N = 19) (upper right-hand plot). Triangles represent the times for  
670 which propagation speed and water vapor convergence values were calculated  
671 (See Table 1 and text). Bottom plots show cloud top temperature (degrees K,  
672 ranging from 245K (blue) to 305K(red)) at 12:30pm local time for convective  
673 (bottom left-hand plot) and non-convective (upper right-hand plot) days. 31
- 674 4 Plot of diurnal cycle of PWV as a function of both season and location for  
675 Manaus stations: ZF29, JPL6, CHR5 and HORT representing a forest, inte-  
676 rior and river sites, respectively (See Figure 2). The blue solid lines represent  
677 the wet season, black short dashed lines, the dry-to-wet transition and red  
678 long dashed, the dry season. 32
- 679 5 Photos of ADGMN sites. Upper left-hand is Manaus station ZF29, upper  
680 right-hand is Manaus station HORT, bottom left-hand is Manaus station  
681 CTLO and bottom right-hand is Belem station BJRN. 33

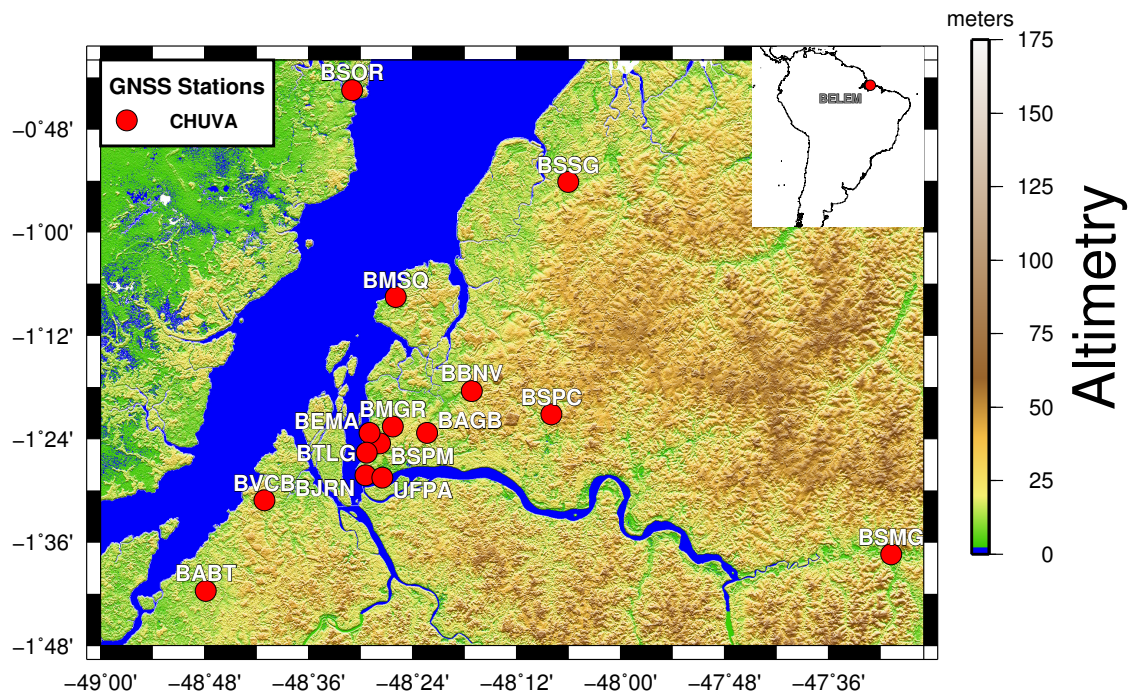


FIG. 1. Map of the Belem Dense GNSS Meteorological Network during the CHUVA experiment June 2011. Sounding sites were BSMG and BSSE (near BEMA). Tomé Açu is to the south of the mapped region. The large water body west of Belem is the Bahia de Marajó.

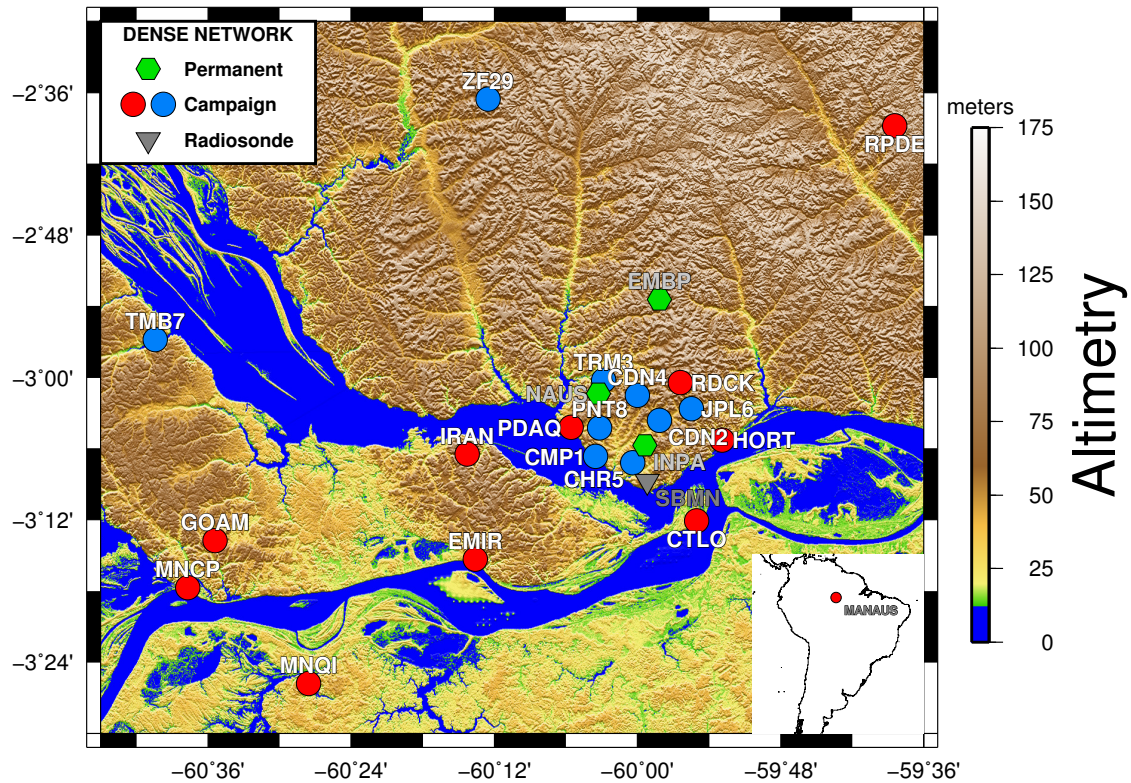


FIG. 2. Map of the Manaus Dense GNSS Meteorological Network, April 2011 - April 2012. Green and blue stations were present for the duration of the experiment. Red stations were present from August 2011 to April 2012. SBMN (82332) is the site for twice daily radiosondes and represents the tip of the Manaus “peninsula”.

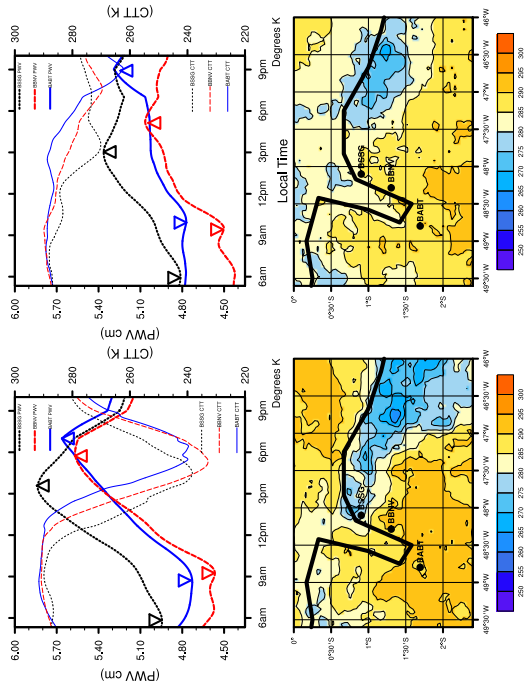


FIG. 3. Plot of timeseries of average PWV (every 5 minutes) BSSG (black,short dash), BBNV(red, long dash) and BBT(blue, solid) and average cloud top temperature (CTT) (every 15 minutes) (Identical patterns and colors, but thinner lines) for convective days ( $N = 22$ ) (upper left-hand plot) and non-convective days ( $N = 19$ ) (upper right-hand plot). Triangles represent the times for which propagation speed and water vapor convergence values were calculated (See Table 1 and text). Bottom plots show cloud top temperature (degrees K, ranging from 245K (blue) to 305K (red)) at 12:30pm local time for convective (bottom left-hand plot) and non-convective (upper right-hand plot) days.

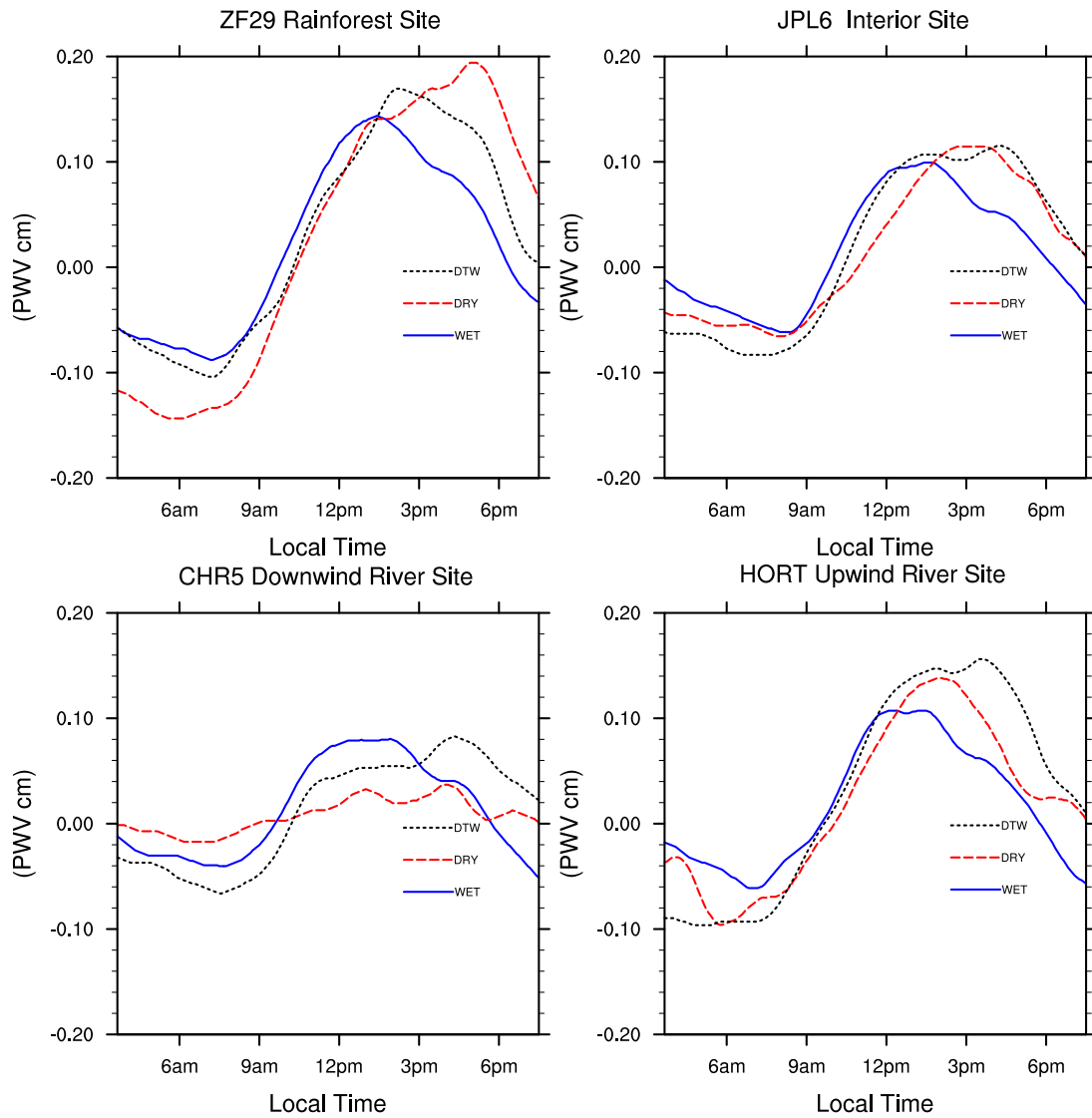


FIG. 4. Plot of diurnal cycle of PWV as a function of both season and location for Manaus stations: ZF29, JPL6, CHR5 and HORT representing a forest, interior and river sites, respectively (See Figure 2). The blue solid lines represent the wet season, black short dashed lines, the dry-to-wet transition and red long dashed, the dry season.



FIG. 5. Photos of ADGMN sites. Upper left-hand is Manaus station ZF29, upper right-hand is Manaus station HORT, bottom left-hand is Manaus station CTLO and bottom right-hand is Belem station BJRN.